A Kinetic Model for Sulfur Accelerated Vulcanization of a Natural Rubber Compound

R. DING and A. I. LEONOV*

Polymer Engineering Department, The University of Akron, Akron, Ohio 44325

SYNOPSIS

Vulcanization kinetics for a natural rubber compound were studied by a kinetic approach using the cure meter and DSC methods. A simplified but realistic model reaction scheme was used to simulate induction, curing, and overcure periods continuously. Physically significant parameters of the model were extracted from isothermal experimental data using a cure meter. The calculation demonstrated a good correspondence with isothermal cure meter data over the temperature range studied. The length of induction time, variation of maximum modulus with temperature, and the reversion phenomena observed from cure curves can be predicted. DSC data were found to be incompatible with the cure meter test, because the complex vulcanization reaction system is multiexothermal and it is difficult to isolate the heat due to crosslinking. Hence, the cure meter technique is suggested for the study of crosslink formation. The kinetic approach provides a way to incorporate vulcanization kinetics into simulation of reactive processing operations. © 1996 John Wiley & Sons, Inc.

INTRODUCTION

To model a reactive processing operation it is necessary to obtain complete kinetic, thermal, and rheological characterization of the material during reaction, because in addition to temperature and shear rate, thermal and rheological properties depend on the degree of reaction. Hence, determination of the reaction kinetics becomes very important.

The phenomenological approach was employed first by the application of the so-called general form of macrokinetics.[1-5] With increased understanding of the nature of the reaction, more attention has been paid to the kinetic approach. The related research is largely in the area of application of the kinetic approach to the study of thermosetting polymer systems for the purposes of reactive injection molding, pultrusion, and sheet molding compound operations.[6-10] Most of these systems follow the free radical polymerization mechanism. However, the phenomenological approach still dominates the study of rubber vulcanization in academic and industrial areas, with very few publications using the kinetic approach. The main difficulty includes the lack of complex details regarding the reaction chemistry. Also, an appropriate way of simplifying the complex reaction systems to facilitate easy numerical calculation has not been established.

Popular techniques used to study rubber vulcanization include differential scanning calorimetry (DSC), oscillating disk rheometry (cure meter), and chemical analysis. The DSC technique is based on the assumption that the heat of reaction is only due to the crosslinking reaction and is proportional to the extent of the reaction. This is questionable for a complex reaction system. The cure meter is based on the fact that the crosslinking density is proportional to the stiffness of the rubber. Usually, the degree of cure can be defined for DSC and cure meter techniques, respectively, as follows:

$$X = \Delta H_t / \Delta H_\infty \tag{1}$$

$$X = (G'_t - G'_0)/(G'_\infty - G'_0). \tag{2}$$

Here X is the degree of cure, ΔH_t is the cumulative heat evolved up to time t, and ΔH_∞ is the total

* To whom correspondence should be addressed.

Journal of Applied Polymer Science, Vol. 61, 455–463 (1996)
 CCC 0021-8995/96/030455-09

amount of heat generated during the entire reaction. G'_t is the storage modulus at the conditions corresponding to the time t, G'_0 is the initial storage modulus, and G'_∞ is the storage modulus at the end of the curing reaction.

Three main regions of cure can be distinguished in the cure curve for a typical accelerated sulfur vulcanization process (Fig. 1). First there is a scorch delay or induction period that provides a safe processing time. It is believed that the accelerator chemistry is mostly involved in this period. The second region is the curing period, during which network structure is formed. The third period maturates the network by overcure during which reversion, equilibrium, and increasing characteristics can be found for different compounds.

The phenomenological approach to the cure kinetics was reviewed in the literature.[11,12] The cure curve is the basis for kinetics study using the phenomenological approach. Because reaction in the induction period behaves differently from the curing period, one has to describe the cure curve separately. An Arrhenius type relation is frequently employed to describe induction time. In the isothermal case, the relation can be written as

$$t_i = a \exp(-b/T), \tag{3}$$

where t_i is induction time, a and b are material constants, and T is absolute temperature. In the nonisothermal case, induction time is implicitly expressed by an integral equation,

$$\int_0^{t_i} \frac{d\tau}{t_i(T(\tau))} = 1, \tag{4}$$

where t_i takes the form of eq. (3) and τ is a dummy time variable. With eq. (4), obtaining the substantial derivative of the extent of reaction becomes very difficult.

For the curing period, an S-shaped cure curve is often observed, which indicates the autoaccelerated reaction characteristics. A general form of macrokinetics can be applied for this period.

$$dX/dt = K(T) \cdot f(X), \tag{5}$$

where

$$K(T) = k_0 \cdot \exp(-E/RT), \tag{6}$$

and

$$f(X) = X^m(1 - X)^n. \tag{7}$$

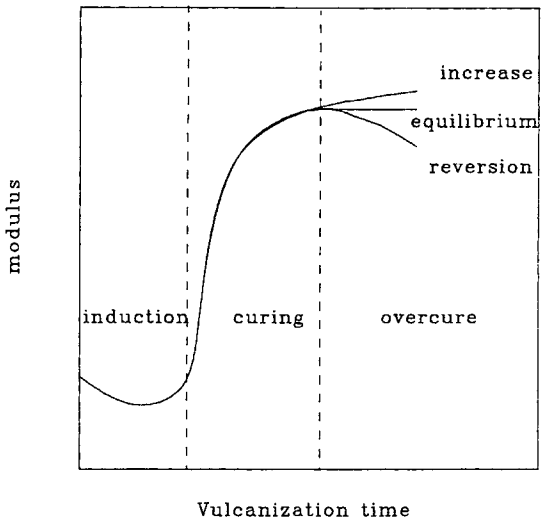

Figure 1 A typical accelerated sulfur vulcanization cure curve obtained from a cure meter.

A specific example of four-parameter macrokinetics can be given as[4]

$$dX/dt = (K_1 + K_2X^m)(1 - X)^n. \tag{5a}$$

It should be noted that a lot of freedom exists in the determination of the number of model parameters and in the specification of a particular form of macrokinetics.

A more detailed kinetic approach requires the knowledge of vulcanization chemistry so that a proper model reaction scheme can be obtained. A complex model representation of the reaction will result in a set of nonlinear differential equations. Appropriate assumptions and simplifications are usually made to achieve an easy numerical solution in most practical cases. Kinetic parameters are often obtained through a nonlinear curve fitting routine.

Important advantages of a kinetic approach over a phenomenological one are: the kinetic approach is based on a better understanding of the reaction mechanism and provides certain physical sense; this approach is able to simulate the vulcanization process as a whole; it provides a possible way to relate process conditions, product structure, and properties directly to the compound formulation; and it can be incorporated into reactive processing simulation for a moving medium. Still, for systems that are very complex and lacking in the knowledge of chemistry, the phenomenological approach is the most practical method.

The study of the mechanism of accelerated sulfur vulcanization dates back to 1946. Many reaction schemes have been proposed since the early 1960s. A good early review was given by Bateman et al.[13]

A recent review of sulfur crosslinking fundamentals for accelerated and unaccelerated vulcanization was published by Krejsa and Koenig.[14] The general course of vulcanization is described as follows.

First, an active accelerator complex is formed by some prior interaction of accelerator and activator with the presence of soluble zinc. This complex can react with molecular sulfur to form a sulfurating agent. One of the mechanisms of the fission of an S_8 ring is due to attack by nucleophilic sulfur atoms of accelerator complexes.[13] Existence of these complexes was detected chemically[15,16] and also by the combined NMR/HPLC analysis.[17]

Second, a sulfurating agent can react with rubber chains to form a crosslinking precursor. The precursor was identified by experiment evidence[18,19] as an accelerator-terminated polysulfidic pendant group attached to the rubber chain.

Precursors subsequently undergo the formation of polysulfidic crosslinks. In the mean time, loss of crosslinking efficiency may also take place due to the decomposition and desulfuration of precursors.[18,20] Because of the side reactions, formation of cyclic sulfide, conjugated dienes, trienes, ZnS, and a monosulfidic pendant group could be observed. These resulting species are not able to contribute to crosslinks. It was found that the activity, concentration of zinc-accelerator complexes,[19,21] and temperature play the central role of competition between the above possible reaction routes.

Finally, the initially formed network matures during which similar desulfuration (crosslink shortening, eventually leading to monosulfidic crosslinks) and decomposition of polysulfidic crosslinks takes place. In addition, a sulfur exchange reaction mechanism was proposed[22,23] for the desulfuration process.

Based on Krejsa et al.,[17] an overall scheme of vulcanization is shown in Figure 2 where key reaction steps are summarized. It is noticed that during the curing and network maturing periods, at least three reactions are in competition, namely, crosslinking, desulfuration, and decomposition reactions. The balance of reactions is not only dependent on the temperature but also on accelerator type and its concentration.

A simplified kinetic scheme (I) for accelerated sulfur vulcanization is according to Coran[24]:

$$A \xrightarrow{k_1} B \xrightarrow{k_2} B^* \xrightarrow{k_3} \alpha Vu$$
$$A + B^* \xrightarrow{k_4} \beta B \qquad \text{(I)}$$

where A is the accelerator and/or its reaction products (with sulfur, Zn++, etc.); B is a precursor to

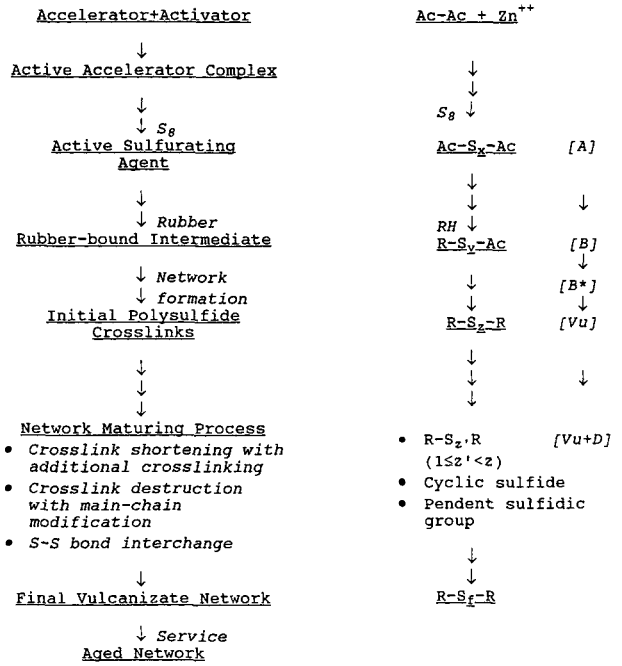

Figure 2 General reaction scheme for accelerated sulfur vulcanization.

crosslinks, probably polymeric; B^* is an activated form of B, such as a polymeric polythiyl radical; Vu is a crosslink; and α and β are adjustable stoichiometric parameters. It was considered that if the reaction through k_4 is much faster than through k_3, crosslink precursors B^* are rapidly quenched. Crosslinking formation would be impeded until A is substantially depleted. It is also considered that k_4 and k_3 are much greater than k_1 and k_2. With this scheme and assumptions, under isothermal conditions, Coran[24] described the induction period kinetically rather than using an Arrhenius type relationship. The curing period was described separately by simple first-order kinetics.

Scheme (I) provides for an induction mechanism and is able to describe the induction, curing, and overcure (with equilibrium character) periods continuously. However, it cannot explain the change of maximum modulus with temperature, which was observed from the vulcanization of an styrene-butadiene rubber (SBR) compound.[25] It was considered that, in addition to the crosslinking reaction, competitive side reactions that produce inactive species coexist. Therefore, scheme (I) was modified by adding a side reaction[25]:

$$A \xrightarrow{k_1} B \xrightarrow{k_2} B^* \xrightarrow{k_3} \alpha Vu$$
$$B^* \xrightarrow{k_5} \gamma D$$
$$A + B^* \xrightarrow{k_4} \beta B \qquad \text{(II)}$$

where D represents inactive side products. Thus scheme (II) introduces a competition between main reactions and side reactions, which can be regulated by temperature T to establish a change of crosslink density with curing temperature.

It is noted that scheme (II) is limited to those sulfur accelerated vulcanization systems with equilibrium overcure characteristics. However, for natural rubber (NR) rubber, reversion in the overcure period is a typical observation. Our objective was to achieve a kinetic description of a NR vulcanization process under isothermal and nonisothermal conditions.

KINETIC MODEL

Scheme (II) was successfully used to predict the SBR vulcanization process having equilibrium overcure. To describe reversion, in addition to the main reaction (crosslinking) and the parallel competitive side reaction, a consecutive crosslinks decomposition reaction, which also produces inactive species (such as pendant sulfur branches and/or cyclic sulfur in rubber backbones), needs to be considered. This consecutive decomposition reaction takes place during curing and overcuring periods. Therefore, scheme (II) can be modified as follows:

$$\begin{aligned} A \xrightarrow{k_1} B \xrightarrow{k_2} B^* \xrightarrow{k_3} \alpha Vu \\ Vu \xrightarrow{k_6} \gamma D \\ B^* \xrightarrow{k_5} \gamma D \\ A + B^* \xrightarrow{k_4} \beta B \end{aligned} \qquad \text{(III)}$$

where D is inactive side products. It is noted that scheme (III) not only introduces competition between the main reaction and side reaction, which can be regulated by temperature, but also provides a reversion overcure due to the consecutive reaction through k_6.

Based on scheme (III), rate equations and a mass balance may be written as

$$dA/dt = -k_1A - k_4AB^* \tag{8a}$$

$$dB/dt = k_1A - k_2B + \beta k_4AB^* \tag{8b}$$

$$dB^*/dt = k_2B - k_4AB^* - (k_3 + k_5)B^* \tag{8c}$$

$$d(Vu/\alpha)/dt = k_3B^* - (1/\alpha)k_6Vu \tag{8d}$$

$$d(D/\gamma)/dt = k_5B^* + k_6Vu, \tag{8e}$$

with initial conditions

$$A\ (t = 0) = A_0; \quad B\ (t = 0) = 0;$$
$$Vu\ (t = 0) = 0; \quad D\ (t = 0) = 0; \tag{9}$$

and the mass balance equation

$$A_0 = A + B + B^* + Vu/\alpha + D/\gamma. \tag{10}$$

Equations (8) and (10) lead to the result

$$\alpha = 1, \quad \beta = 2.$$

For the sake of simplicity, we use notation D instead of D/γ in the rest of this article.

When applying the quasi-steady-state approximation on B^* and assuming that

$$k_2/k_3 \ll 1, \quad k_4/k_3 = \phi, \quad k_5/k_3 = \psi, \tag{11a-c}$$

the final set takes the form

$$\frac{dA}{dt} = -k_1A - \frac{\phi k_2A(A_0 - A - Vu - D)}{1 + \psi + \phi A} \tag{12}$$

$$\frac{dB}{dt} = k_1A - \frac{k_2(1 + \psi - \phi A)(A_0 - A - Vu - D)}{1 + \psi + \phi A} \tag{13}$$

$$\frac{dVu}{dt} = \frac{k_2(A_0 - A - Vu - D)}{1 + \psi + \phi A} - k_6Vu \tag{14}$$

$$\frac{dD}{dt} = \frac{\psi k_2(A_0 - A - Vu - D)}{1 + \psi + \phi A} + k_6Vu. \tag{15}$$

Under isothermal conditions with species A being completely consumed ($A \to 0$), summation of eqs. (14) and (15) yields

$$dP/dt = k_2(A_0 - P) \quad \text{for } t \geq t_i \tag{16}$$

with $P\ (t = t_i) = 0$ where $P = Vu + D$ and $t_i = t(A \to 0)$. The above initial condition is due to the approximation that curing reaction will not start until A is depleted at time t_i (induction time). The solution of eq. (16) is

$$P = A_0[1 - \exp(-k_2t')], \tag{17}$$

where $t' = t - t_i$. Substituting eq. (17) into (14) gives

$$dVu/dt' = A_0k_2[\exp(-k_2t')]/(1 + \psi) - k_6Vu$$
$$Vu\ (t' = 0) = 0. \tag{18}$$

The solution of (18) can be written as:

$$Vu = A_0 k_2[\exp(-k_2 t') - \exp(-k_6 t')]/[(1 + \psi)(k_6 - k_2)]. \quad (19)$$

Consider the maximum cure at $t = t_m$ or $t' = t_m - t_i$. We have

$$dVu/dt' = 0, \quad \text{at} \quad t' = t_m - t_i, \quad (20)$$

which leads to

$$t_m - t_i = \frac{\ln k_2/k_6}{k_2 - k_6}. \quad (21)$$

In the final set, eq. set (12)–(15), there are five fitting parameters. The fitting procedure using isothermal data is as follows: first, using eqs. (19) and (21), k_2 and ψ can be obtained by knowing two characteristic points on the cure curve, say the maximum point and a point in the overcure region (in the decreasing branch after maximum). Then, k_6 is automatically calculated due to eq. (21). k_1 and ϕ can be determined from induction time and the initial slope of the cure curve in the curing period.

Because rate constant k_i (i = 1, 2, 6) and the ψ parameter take the forms

$$k_i = k_{i0}\exp(-E_i/RT) \quad (22)$$

$$\psi = a \exp(b/T), \quad (23)$$

their temperature dependence can be obtained by doing cure meter experiments at three different temperatures.

EXPERIMENTAL

An oil extended and carbon black filled NR compound was used for the study of vulcanization kinetics. The compound was stored in a freezer at about −15°C before testing. Its formulation is laid out in Table I.

Table I Recipes for NR compound

Ingredient	NR (phr)
NR (SMR5L)	100
Carbon black	82
Aromatic oil	54
Zinc oxide	5
Stearic acid	2
Antioxidant	2
Sulfur	2.5
Santocure®	0.6

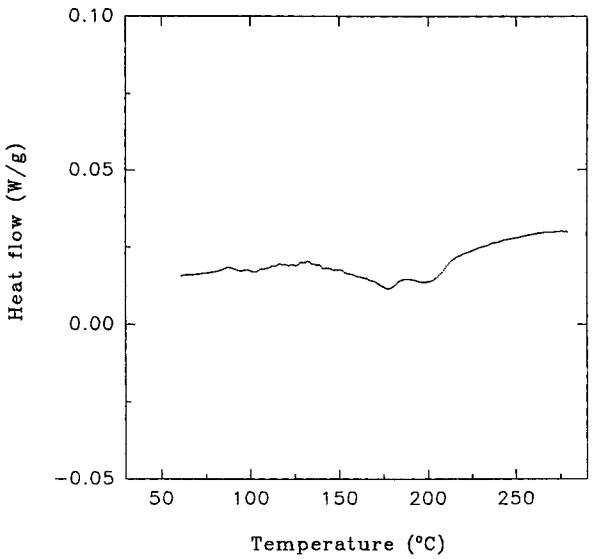

Figure 3 A typical trace of a DSC thermogram obtained at 10°C/min heating rate for NR compound.

Vulcanization of NR samples was conducted in a DSC (Perkin–Elmer DSC-7) under nonisothermal conditions in a nitrogen atmosphere. DSC scans were made at fixed heating rates of 10, 12.5, and 15°C/min within the temperature range of 30–280°C. A typical DSC trace is shown in Figure 3 where two overlapped peaks are observed. An isothermal DSC run was not employed here because the isothermal reaction peak is too small and too broad to be determined accurately.

Isothermal vulcanization of NR was readily performed using a cure meter (RPA 2000). Samples underwent a dynamic oscillation at 1% strain amplitude and 1-Hz frequency. Isothermal temperatures were 130, 140, and 150°C, respectively. Their cure curves are shown in Figure 4 in terms of storage modulus.

RESULTS AND DISCUSSION

There are five temperature-dependent parameters with certain physical meanings in the kinetic model. The parameter k_2 is a function of temperature and controls the rate of cure, especially in the late stage of the curing period. Higher values of k_2 indicate a faster rate of cure. The parameter ψ partially regulates the competition between crosslinking and side reactions by temperature. It causes a change of the maximum crosslink density with process temperature. Lower vulcanization temperature results in a higher maximum crosslink density. The rate constant k_6 also affects the maximum cure and changes reversion rate in the overcure period. Because the

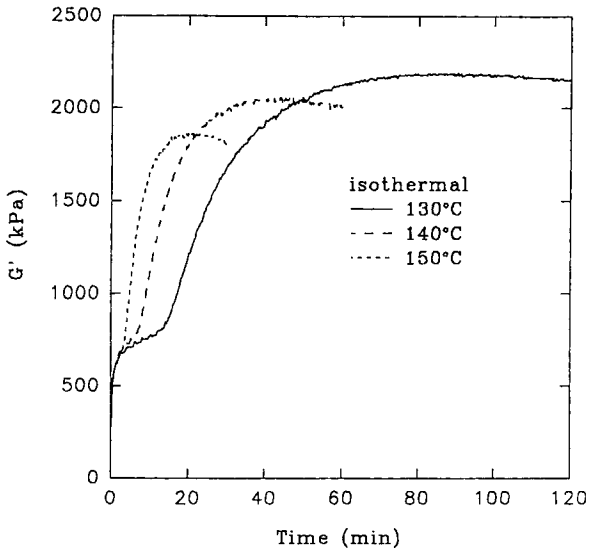

Figure 4 NR cure curves obtained from a cure meter under various isothermal conditions.

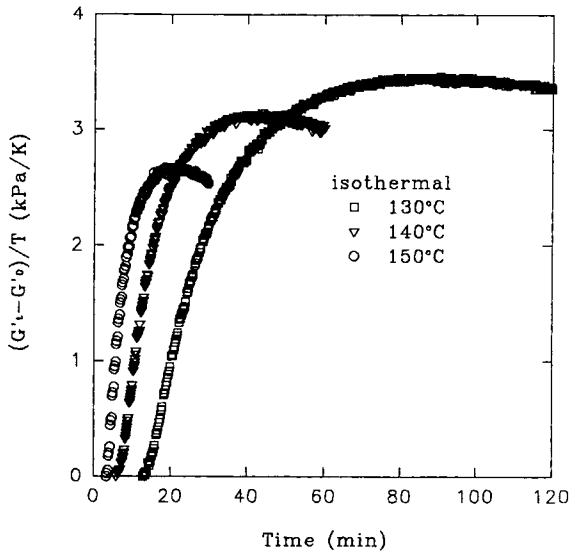

Figure 5 The equilibrium quantity of $(\Delta G'/T)$ varies with isothermal cure temperature for the NR compound.

main reaction, parallel side reaction, and consecutive side reaction take place simultaneously, the above-mentioned three model parameters control the curing and overcure periods. The parameter k_1 is temperature dependent and mainly determines the induction time. Larger values of k_1 result in a shorter induction time. The parameter ϕ characterizes the initial rate of curing reaction immediately after the induction period, and is observed to be insensitive to temperature. A larger value of ϕ gives a more rapid transition from scorch to curing.

All model parameters for accelerated sulfur vulcanization of NR were fitted based on cure meter data and are listed in Table II.

The first interesting observation is the plot of the quantity $\Delta G'/T$ against time, which is shown in Figure 5. It can be seen that the quantity $\Delta G'/T$, which is proportional to the number of crosslinks according to rubber elasticity, at maximum cure varies with curing temperature. This might be explained by introducing the side reactions that compete with the formation of crosslinks, where the competition is influenced by the temperature. Therefore, similar to model reaction scheme (II), parameter ψ is introduced by addition of the parallel reaction through k_5, and parameter k_6 is added due to the consecutive decomposition reaction.

With fitting parameters, comparisons between the model calculations and isothermal cure meter data are shown in Figure 6. Model calculations continuously simulate the induction, curing, and reversion periods of the NR vulcanization process. They achieve good agreement with experimental data over the temperature range studied.

In Figure 7, the model simulates the change of concentration for each species during the course of vulcanization. With this knowledge, one may design a proper temperature profile to obtain an optimal vulcanization condition. Also it helps to study the kinetics and compound formulations. How each parameter in the model affects the cure curve will be demonstrated below.

Figure 8 shows the effect of ϕ value on the rate of cure. It can be seen that the change of ϕ value almost does not influence the late stage of cure. However, an increase in ϕ value sharpens the initial slope of the curing period, which results in a more effective delay. Because ϕ is the ratio of k_4 to k_3, and the scorch delay is due to the competition of reactions through k_4 and k_3, it is obvious that a larger

Table II Model Parameters of Scheme (III)

	k_{10} (1/min)	E_1 (J/mol)	k_{20} (1/min)	E_2 (J/mol)	k_{60} (1/min)	E_6 (J/mol)	ϕ $(\text{mol/m}^3)^{-1}$	a	b (K)
NR	8.926×10^{12}	1.073×10^5	1.248×10^{10}	8.789×10^4	4.447×10^{16}	1.507×10^5	400	2477.0	−1432.6

Parameters from isothermal curemeter experiment for accelarated sulfur vulcanization of NR compound.

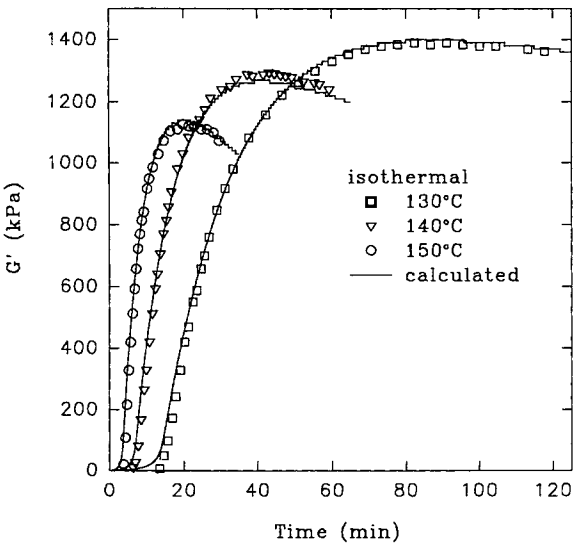

Figure 6 Comparison of model calculated cure curve and cure meter data under various isothermal conditions.

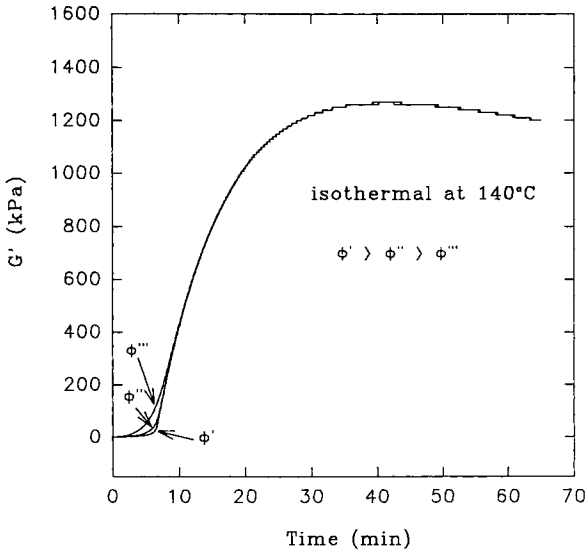

Figure 8 Effect of parameter ϕ on the initial rate of cure.

value of ϕ will lead to a more effective and longer induction period.

The rate constant k_1 seems only to influence the length of induction time in Figure 9. With a decrease in k_1, the whole cure curve shifts to the right to give a longer delay period. The value of k_1 is determined by the nature of the given accelerator system in addition to its concentration and temperature.

Figure 10 shows the effect of k_2 (through which crosslinks are generated) on the cure curve. Change in the value of k_2 does not greatly affect the induction time. However, it affects the slope of the cure curve, especially in the later stage of cure. With a decrease in k_2 value, the rate of cure and maximum modulus decrease and the maximum cure time increases.

Figure 11 simulates the change of modulus with the parameter ψ. Because ψ is the ratio of k_5 and k_3, higher ψ value favors the parallel side reaction and results in a lower crosslinking density. In addition to the temperature, the parameter ψ is also determined by the accelerator type and its concentration.

Reversion phenomena are demonstrated in Figure 12. Due to the decomposition of crosslinks through k_6, modulus decreases after it reaches a maximum.

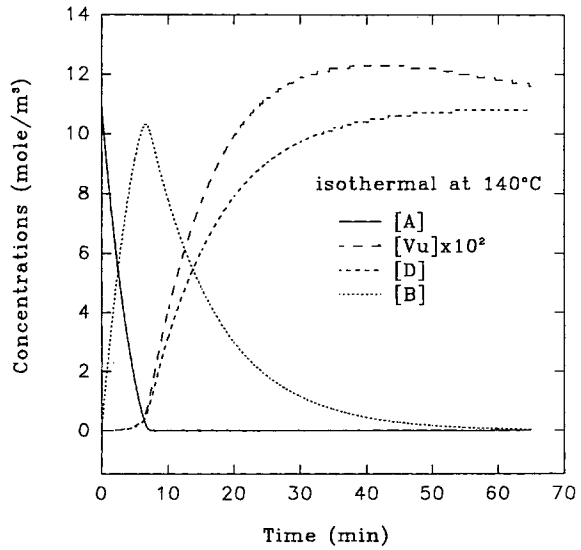

Figure 7 Change of concentration of each species during the course of vulcanization.

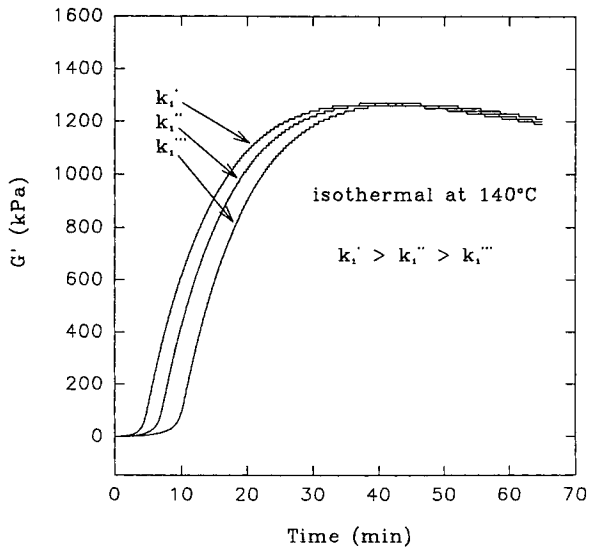

Figure 9 Effect of model parameter k_1 on the induction time.

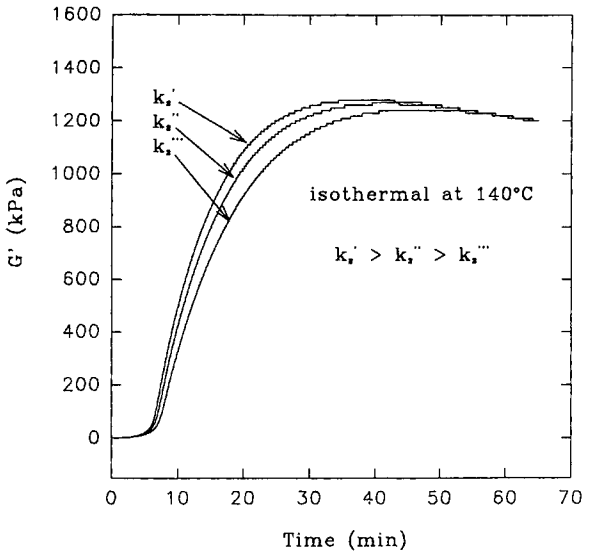

Figure 10 Effect of model parameter k_2 on the rate of cure.

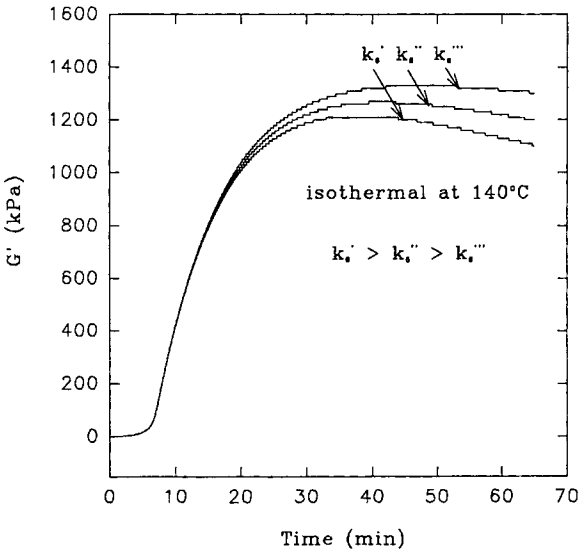

Figure 12 Effect of model parameter k_6 on the rate of reversion.

Higher k_6 value leads to an earlier occurrence of reversion and a faster reversion rate.

Reaction behavior in the curing period is controlled by k_2, k_6, and ψ together. Temperature is the most important adjustable control variable that balances these three model parameters. Desired curing rate, maximum crosslink density, maximum cure time, and reversion rate could be achieved by optimization of process conditions.

Predicted rate of heat generation, due to the curing reaction in the nonisothermal case, is compared with DSC experimental data shown in Figure 13. The rate of heat generation during DSC scanning is obtained by differentiating the degree of heat generation curve. It is seen that the model-predicted induction time is longer than the time when heat is initially generated. It seems that the first peak in the DSC trace corresponds to the curing reaction, whereas the side reaction contributes partially to both peaks. Because the disagreement is apparent in both the time domain and the peak's shape, similar to our result obtained from the study of SBR vulcanization, it might be explained that the DSC technique measures total heat generation during vulcanization, including all possible exothermal re-

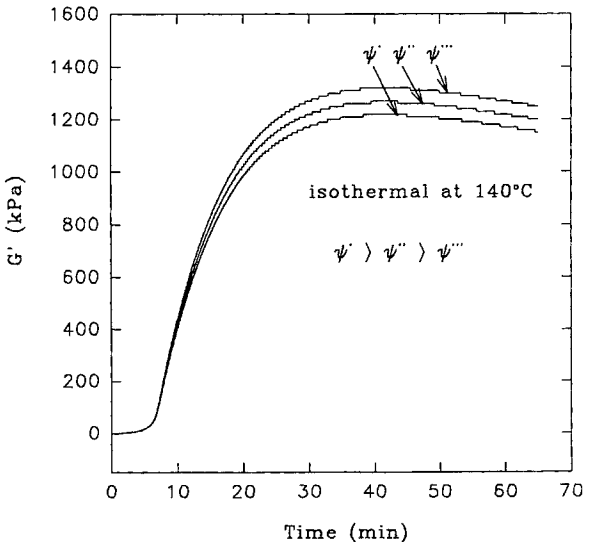

Figure 11 Effect of model parameter ψ on the crosslinking density.

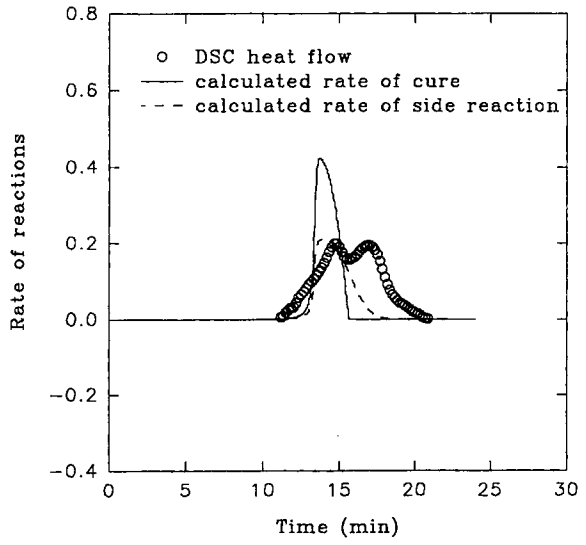

Figure 13 Comparison between model calculations and DSC data under nonisothermal conditions (10°C/min heating rate).

actions that, unfortunately, are not separable. On the other hand, the model calculation is based on cure meter experiments that measure the number of crosslinks formed regardless of the amount of heat released during the reaction. Hence, it can be concluded that the above-mentioned two techniques are not compatible. If one could distinguish the DSC heat peaks from different reactions, hopefully our kinetic model would be able to describe the part of the heat events that corresponds to the crosslink formation reaction during vulcanization.

CONCLUSIONS

1. Instead of the phenomenological approach, a kinetic approach is used to simulate the accelerated sulfur vulcanization of NR from induction, curing, and overcure. This enables us to incorporate vulcanization kinetics into processing simulation of moving reactive media, therefore, to control and to optimize the processing operation.
2. The model reaction scheme used in this study seems simple and realistic. It provides a mechanism for scorch delay, explains the variation of maximum crosslink density with temperature, and predicts the reversion phenomena for the given compound.
3. Model calculations show good agreement with isothermal cure meter experimental data over the studied temperature range.
4. When compared with nonisothermal DSC data, the predicted cure curve based on the cure meter technique is different from the heat flow trace. This might lead to the conclusion that the cure meter and the DSC techniques are not compatible. Reaction heat from DSC does not have a simple correspondence to the generation of crosslinks observed from the cure meter. For the system with multiexothermal reactions, for example, accelerated sulfur SBR and NR vulcanization, the cure meter technique is more reliable than DSC.

REFERENCES

1. A. I. Leonov and A. I. Schwarz, *Polym. Sci., U.S.S.R.,* **3,** 778 (1972).
2. G. Gyulai and E. J. Greenhow, *Thermochim. Acta,* **5,** 481 (1973).
3. K. Horie, H. Hiura, M. Sawada, I. Mita, and H. Kambe, *J. Polym. Sci.,* **8,** 1357 (1970).
4. M. R. Kamal, S. Sourour, and M. Ryan, *SPE ANTEC Tech. Papers,* **19,** 187 (1973).
5. A. Ya. Malkin, V. G. Frolov, A. N. Ivanova, and Z. S. Andrianova, *Polym. Sci. U.S.S.R.,* **21,** 691 (1979).
6. G. L. Batch and C. W. Macosco, *SPE ANTEC Tech. Papers,* **1,** 974 (1987).
7. J. F. Stevenson, *SPE ANTEC Tech. Papers,* **26,** 452 (1980).
8. J. F. Stevenson, *Polym. Process Eng.,* **1,** 203 (1984).
9. L. J. Lee, *Polym. Eng. Sci.,* **21,** 483 (1981).
10. G. L. Batch, C. W. Macosco, and D. N. Kemp, *Rubber Chem. Technol.,* **64,** 218 (1991).
11. T. W. Chan, G. D. Shyu, and A. I. Isayev, *Rubber Chem. Technol.,* **66,** 849 (1993).
12. A. I. Isayev and J. S. Deng, *Rubber Chem. Technol.,* **61,** 340 (1988).
13. L. Bateman, C. G. Moore, M. Porter, and B. Saville, in *The Chemistry and Physics of Rubber-Like Substances,* L. Bateman, Ed., Maclaren and Sons Ltd., London, 1963, Chap. 15.
14. M. R. Krejsa and J. L. Koenig, *Rubber Chem. Sci.,* **66,** 376 (1993).
15. R. H. Campbell and R. W. Wise, *Rubber Chem. Technol.,* **37,** 635 (1964).
16. A. Y. Coran, *Rubber Chem. Technol.,* **37,** 679 (1964).
17. M. R. Krejsa, J. L. Koenig, and A. B. Sullivan, *Rubber Chem. Technol.,* **67,** 348 (1994).
18. D. S. Campbell, *J. Appl. Polym. Sci.,* **14,** 1409 (1970).
19. C. R. Parks, D. K. Parker, D. A. Chapman, and W. L. Cox, *Rubber Chem. Technol.,* **43,** 572 (1970).
20. N. J. Morrison and M. Porter, *Rubber Chem. Technol.,* **57,** 63 (1984).
21. C. R. Parks, D. K. Parker, and D. A. Chapman, *Rubber Chem. Technol.,* **45,** 467 (1972).
22. B. Milligan, *Rubber Chem. Technol.,* **39,** 1115 (1966).
23. R. W. Layer, *Rubber Chem. Technol.,* **65,** 211 (1992).
24. A. Y. Coran, *Rubber Chem. Technol.,* **37,** 689 (1964).
25. R. Ding, A. I. Leonov, and A. Y. Coran, *Rubber Chem. Technol.,* **69,** 81 (1996).

Received September 21, 1995
Accepted November 7, 1995